Published in final edited form as:
Dev Dyn. 2012 April ; 241(4): 759–769. doi:10.1002/dvdy.23749.

Roundabout is required in the Visceral Mesoderm for Proper Microvillus Length in the Hindgut Epithelium

Nadine H. Soplop[1,2], **Yi-Shan Cheng**[1], and **Sunita G. Kramer**[1,2,*]

[1]Department of Pathology and Laboratory Medicine Robert Wood Johnson Medical School, University of Medicine and Dentistry of New Jersey, 675 Hoes Lane Piscataway, NJ 08854, Phone: (732) 235-4226 Fax: (732) 235-4825

[2]Graduate Program in Cell and Developmental Biology UMDNJ-Graduate School of Biomedical Sciences & Rutgers: The State University of New Jersey 190 Frelinghuysen Road Piscataway, NJ 08854-8020

Abstract

In this study we examined Roundabout signaling in the *Drosophila* embryonic hindgut. Slit and its receptors Roundabout (Robo) and Roundabout 2 (Robo2) localize to discrete regions in the hindgut epithelium and surrounding visceral mesoderm. Loss of *robo, robo2 or slit* did not disrupt overall hindgut patterning. However *slit* and *robo* mutants showed a decrease in microvillus length on the boundary cells of the hindgut epithelium. Rescue and overexpression analysis revealed that *robo* is specifically required in the visceral mesoderm for correct microvillus length in the underlying hindgut epithelium. Expression of *robo* in the visceral mesoderm of *robo* mutant embryos restored normal microvillus length, while overexpression of *robo* resulted in an increase in microvillus length. Microvillus length was also increased in *robo2* mutants suggesting that *robo2* may antagonize *robo* function in the hindgut. Together, these results establish a novel, dose-dependent role for Robo in regulating microvilli growth and provide *in vivo* evidence for the role of the visceral mesoderm in controlling morphological changes in the underlying intestinal epithelium.

Keywords

Drosophila; hindgut development; microvillus; Robo; Slit

INTRODUCTION

The *Drosophila* hindgut (HG) is the most posterior segment of the alimentary canal that originates from the invagination of ectodermal cells to form a single cell layer epithelial tube surrounded with visceral mesoderm (Skaer, 1993; Campos-Ortega and Hartenstein, 1997). At stage 13 of embryogenesis, the HG has adopted its characteristic sigmoidal shape and when fully developed at stage 16, consists of three regions along the anteroposterior axis: the small intestine, large intestine and rectum (for review see (Lengyel and Iwaki, 2002)) (Fig. 1A). The large intestine (LI) is the only portion of the HG that also forms three distinct regions along the dorsal-ventral axis, which are distinguished both by their morphology (Fig. 1A, S1A,E,I) as well as gene expression patterns. Expression of Engrailed specifies the dorsal cells (Fig. S1A) that become specialized for ion and water absorption (Murakami and Shiotsuki, 2001). The ventral cells are identified by being Engrailed-negative and Delta

*Correspondence: kramersg@umdnj.edu.

positive (Fig S1I). Delta expression in the ventral cells activates the Notch receptor in neighboring dorsal cells (Fig. S1E), inducing their differentiation into two rows of boundary cells (Fuss and Hoch, 2002; Iwaki and Lengyel, 2002; Takashima et al., 2002). Boundary cells (BCs) have an elongated morphology and are distinguished by the presence of organized microvilli on their apical surfaces (Iwaki and Lengyel, 2002). While the molecular pathways required for the establishment of the three cell types in the large intestine have been well established, the mechanisms that are responsible for elaboration of the distinct morphologies of these cell types remain unknown.

Similar to its vertebrate counterpart, the *Drosophila* HG epithelium (HE) is surrounded by a single layer of circular muscles, derived from the hindgut visceral mesoderm (HVM) (Fig. 1A). Multiple lines of evidence reveal a required interaction between the HE and surrounding HVM for their proper specification and development. In *Drosophila*, Wingless signaling from the HE, and perhaps the epidermis, is required to establish and maintain the HE and HVM (Iwaki et al., 2001; San Martin and Bate, 2001; Lengyel and Iwaki, 2002). Signaling from the mesoderm to the epithelium is also important for development, but is less understood (for review see (Lengyel and Iwaki, 2002)). *Drosophila twist* mutants that have defects in HVM development, also show defects in HG morphogenesis (San Martin and Bate, 2001). Similarly, in vertebrates, the requirement for reciprocal endodermal and mesodermal interactions for normal gut development has been known for many years (reviewed by (Roberts, 2000)). These interactions have been shown to be dependent on the secretion of diffusible signaling molecules by both tissue-types. For example, the importance of Hedgehog signaling originating from the epithelium during the development of the visceral mesoderm is well conserved (McLin et al., 2009).

One of the morphological changes in the vertebrate hindgut that has been shown to be dependent upon interactions between the intestinal epithelium and mesoderm is villus formation (reviewed in (Spence et al., 2011)). Intestinal villi are small (~1mm) projections that protrude from the epithelial lining into the lumen of the intestine to increase the surface area available for absorption. Each villus contains multiple microscopic microvilli, which together form the dense brush border on the apical surface of the intestinal epithelia. Microvilli are supported by a bundle of actin filaments that are uniformly oriented so that their “plus” or barbed ends are at the tip of the microvillus protrusion and their “minus” or pointed ends are at the base and anchored into the terminal web that underlies the apical plasma membrane (for reviews see (Bartles, 2000)). During microvilli development, microvilli first assemble into their characteristic shape and then grow in length as the terminal web undergoes stratification creating cortical rigidity at the apical membrane (Heintzelman and Mooseker, 1992). Early grafting studies showed that correct microvilli morphology and expression of brush border enzymes can be induced in intestinal epithelial cells or primary cell cultures prepared from fetal rat intestinal endoderm by association with fetal mesenchyme (Kedinger et al., 1986).

Microvilli are dynamic structures, which undergo constant growth and turnover through actin treadmilling, which allows them to maintain a relatively constant length (for review see (Lin et al., 2005)). Several microvillus-associated proteins have been implicated in the regulation of microvillus assembly and growth. Among them are the F-actin crosslinking proteins fimbrin, villin and espin (reviewed in (Bartles, 2000; Brown and McKnight, 2010) and the ERM proteins ezrin and moesin, which form a link between actin filaments and the plasma membrane (Karagiosis and Ready, 2004; Saotome et al., 2004; Lan et al., 2006). Absence of these proteins leads to shortened and more disorganized microvilli. Furthermore, during early *Drosophila* development, the Abelson kinase was shown to regulate actin polymerization and the absence of Abelson results in excess actin polymerization leading to elongated apical microvilli (Grevengoed et al., 2003). More recently, the transmembrane

cadherin protein Cad99C was shown to localize to microvilli in *Drosophila* follicle cells where it regulates microvillus assembly and length in a concentration-dependent manner (D'Alterio et al., 2005; Schlichting et al., 2006). However while the molecular mechanisms that contribute to microvillus growth in epithelial cells are beginning to be understood, the signals emanating from the mesenchyme that influence epithelial microvillus length, and the mechanisms by which the mesenchyme communicates with the epithelium during this process are not well characterized.

The secreted ligand, Slit, and its receptor, Roundabout (Robo), belong to a highly conserved family of guidance molecules. Initially identified as a repulsive cue for migrating axons during patterning of the *Drosophila* embryonic central nervous system (Rothberg et al., 1990; Kidd et al., 1999; Brose et al., 1999), they are also required to direct other morphogenetic developmental processes, including the patterning of the *Drosophila* embryonic somatic musculature (Kramer et al., 2001), and heart formation where it was discovered that Slit/Robo signaling regulates DE-cadherin localization during heart lumen formation (Santiago-Martinez et al., 2008; Medioni et al., 2008). In this study we examine the function of Robo signaling in *Drosophila* HG development. Our results show that Robo, Robo2 and the ligand Slit are found in the embryonic HE and surrounding HVM. Loss of *robo* results in defects in lumen shape and decrease in microvillus length on BCs. Conversely, overexpression of *robo* in the HVM results in an increase in microvillus length. Loss of robo2 also results in an increase in microvillus length, suggesting that *robo2* may antagonize *robo* function. Furthermore, we show that Robo signaling is specifically required in the surrounding HVM for correct microvillus length in the HE. Together, these results establish a novel, dose-dependent role for Robo signaling in the regulation of microvillus length and provide *in vivo* evidence for the role of the visceral mesoderm in controlling morphological changes in the underlying intestinal epithelium.

RESULTS

Robo, Robo2 and Slit are localized to distinct regions in the hindgut large intestine

We have previously established a role for Slit and Robos during morphogenesis of the *Drosophila* embryonic heart (Santiago-Martinez et al., 2008). In performing these studies, we observed that Slit and Robo proteins also localize to the small and large intestine of the HG and that this localization persists until stage 16, when the HG is fully developed (Fig. 1B,D,F). Our findings for *slit* are consistent with previous studies that reported the expression of *slit* in the embryonic gut and visceral mesoderm (Rothberg et al., 1990; Kraut and Zinn, 2004). Robo and Robo2 are also localized to the regions where the renal (Malpighian) tubules (MTs) (Lengyel and Iwaki, 2002) evaginate from the small intestine at the midgut/hindgut junction (Fig. 1B,D). To more precisely examine the patterns of Slit and Robos in the LI of the HG, we examined embryos that were fixed and stained with anti-Robo, Robo2 or Slit and then cross sectioned and imaged using confocal microscopy (Fig. 1C,C',E,E',G,H). Using this method, we found that Slit and Robo are both localized to the HVM that surrounds the large intestine as well as in intracellular clusters within the cells of the HE (Fig. 1 A,C',H). While Slit and Robo appear to be evenly distributed along the surface of the HVM, Robo2 localization was restricted to the basal surface of the HE, and is enriched specifically in the dorsal cells (Fig. 1A,E'). We did not detect Robo3 protein, a third Roundabout family member (Simpson et al., 2000a) in the HG (data not shown). In addition to Slit staining in the HVM, we also observed strong Slit localization on the apical surface of the BCs of the HE, where microvilli are normally found. We confirmed the BC localization of Slit by double staining with Engrailed, which localizes to the dorsal cell nuclei (Fig. 1H). Interestingly, we failed to detect either Robo or Robo2 on this surface. To examine the distribution of Slit protein on the BCs at higher resolution, we performed immuno-EM on thin sections through the LI (Fig. 1I,J). Slit protein was visualized by

secondary antibodies linked to gold beads. Consistent with our whole mount staining, we observed high levels of electron dense particles on the lumenal surface of the BCs, which correlated in size and shape to microvilli structures.

slit and robo mutants do not have overall defects in specification and size of the HG

To determine whether there were overall HG patterning defects in *slit* and *robo* mutants, we examined the size and shape of the HG in *robo, robo2* and *slit* mutant backgrounds by staining for the transmembrane protein Crumbs (Crb) (Tepass et al., 1990). The anti-Crb antibody strongly labels the entire apical surface of the BCs that run along the length of the LI and that form two rings that form the anterior and posterior borders of the LI (see Fig. 1A) as well as the Malpighian tubules (MTs) (Iwaki et al., 2001; Fuss and Hoch, 2002). We found no significant difference in Crb staining in *slit, robo, or robo2* mutant embryos (Fig. 2B-D) as compared to wild type (Fig. 2A), which indicated that the overall size and shape of the LI was not altered in our mutant backgrounds. Furthermore, the positioning and overall morphology of base of the MTs, which were strongly labeled with Robo and Robo2, were not significantly altered in any of our mutant backgrounds (Fig. 2B-D).

The strong labeling of Crb in the BCs of *slit* and *robo* mutants was an indication that dorsal-ventral patterning occurred properly in the LI and that the BCs were correctly specified (Fuss and Hoch, 2002; Iwaki and Lengyel, 2002; Takashima et al., 2002). To further support this finding, we examined the expression of cell-type specific markers in the LI. The fully developed LI consists of three cell types that are molecularly distinct and can be identified by the expression of Engrailed in the dorsal cells, Delta in the ventral cells and, Notch in the BCs (Fuss and Hoch, 2002; Iwaki and Lengyel, 2002; Takashima et al., 2002). We found no significant alteration of dorsal-ventral patterning of the hindgut in *slit, robo, or robo2* mutants as revealed by Engrailed or Delta staining (Fig. S1 B,C,J,K) (*robo2* data not shown). Furthermore, we found that the Notch-expressing boundary cells, which make microvilli were also properly specified (Fig. S1 F,G).

Together, these findings indicated that *slit* and *robo* are not required for the overall patterning of the HG but rather may play a more specific role in HG morphogenesis. Based on the localization patterns of Slit and Robo proteins in the HVM and HE of the LI, we hypothesized that Slit/Robo signaling could be involved in mediating the interactions between these two tissues. The established role for mesenchymal-epithelial interactions in microvilli formation (Spence et al.; Kedinger et al., 1986; Ratineau et al., 2003), together with the strong localization of Slit protein on the surface of BCs where microvilli form (Fig. 1G') suggested that *slit, robo, and robo2* may be required for microvilli growth or assembly on the BCs of the LI. To further study this possibility, we closely examined LI morphology in cross section using transmission electron microscopy (TEM) in mutant backgrounds.

Characterization of LI morphology in wild type embryos

Because detailed analysis of LI morphology, including that of the BC microvilli has not yet been reported, we first sought to characterize this aspect of wild type cells in the LI. The cells of the LI form a single layer epithelium (HE) that is surrounded by a layer of visceral mesoderm (HVM) (Fig. 3A). By examining transverse sections, we counted 12 +/− 1 cells in the circumference of the stage 16 LI (data is represented as means +/− SE). This number is similar to that previously reported (Iwaki et al., 2001). In addition, the apical surface of the HE is covered by two cuticle layers that are visible by TEM (Murakami and Shiotsuki, 2001) (Fig. 3A'). By following the surface of the cuticle, we measured the length of the apical surface of wild type embryos to be 42 +/− 4μm.

Next, we closely examined the apical surface of BCs in the HE, where the microvilli are found. By TEM, microvilli can be identified on the boundary cells by their uniform shape, uniform periodicity, and visible F-actin bundle (Figure 3A'). Dorsal and ventral cells do not have microvilli, but instead have microvilli-like protrusions. These are distinguishable from microvilli as they are less uniform in shape and periodicity (Fig. 3C). To determine the average length of microvilli on the BCs, we measured microvillus length in TEM sections that were taken at regular intervals along the length of the LI. Specifically, TEM sections of wild type embryos were taken at 100μm, 120μm, 140μm and 160μm from the most posterior point of the embryo (Fig. 1A). The results show that while there is considerable variability in the lengths of an individual microvillus on a boundary cell, the average length stays relatively the same across the length of the hindgut (Fig. 3B). The variability in individual microvillus length is illustrated in box plots (Fig. 5A). All data presented hereafter are taken from TEM sections at or near 100μm. In this region, the average number of microvilli that are visible in a single TEM section is 32 +/− 2 microvilli, and on average, each microvillus is approximately 310+/− 8nm (n=223) in length.

Finally, at the basal surface of the HE cells, close examination of the areas where the HE and HVM are juxtaposed revealed the presence of cellular processes similar to the processes observed between the epithelium and mesenchyme in fetal rat duodenal tissue. These processes have been shown to increase in size and number coincident with microvilli growth (Mathan et al., 1972). Although we cannot discern whether the presence of these processes is causative or correlative to microvilli growth, we did find similar processes in our wild type TEMs at the interface between the HVM and HE (Figure 3D,E). We also observed the presence of junctional complexes, first reported in (Tepass and Hartenstein, 1994) (Fig. 3E), further supporting the idea that these tissues are physically attached and that communication between these tissues may be important for HG development.

robo and *robo2* mutants have defects in microvilli length

Staining with anti-Crb antibody revealed that there were no overall defects in HG shape and size in *slit, robo*, and *robo2* mutants (Fig. 2B-D). We also found by examining TEMs of cross sections that the number of cells in the circumference of the HG was not significantly altered in *slit* or *robo* mutants (12 +/− 1 and 10 +/− 1 respectively). However, we did notice a difference in the shape of the LI lumen in *robo* mutants when we examined embryos in cross-section. Compared to wild type embryos, which have a relatively smooth oval-shaped lumen (Fig. 3A), the lumen of the LI in *robo* mutants was irregular in shape (Fig. 4C). Furthermore, when we measured the length of the apical surface of *robo* mutants, while we often observed an increase over wild type, we did not find these differences to be statistically significant. We did not observe a lumen shape defect in *slit* or *robo2* mutant embryos (Fig. 4A,E).

Next we characterized microvilli number and length in *robo* and *robo2* mutants. We first examined TEM sections of five *robo* mutant embryos. 1/5 of the *robo* TEM sections we examined had severe lumen defects where boundary cells and microvilli could not be identified (data not shown). Of the remaining four embryos, we detected significantly more microvilli on the surface of BCs (44 +/− 5) (Fig. 4C') when compared with wild type (32 +/− 2) ($P = 0.0252$). To evaluate statistical relevance we used un-paired Student t-tests. Biological significance was determined when $P<0.05$ in a two-tailed test. In addition, when we closely examined microvillus size in *robo* mutants, we noticed a reduction in the average length (171 +/− 7nm, n= 175) as compared to wild type (310 +/− 8nm, n=223) ($P< 0.0001$) (Fig. 5). In contrast, *robo2* mutants had less microvilli on BCs (19 +/− 2) (Fig. 4E') and showed an increase in microvillus length as compared to wild type (359 +/−17nm, n=75) ($P = 0.0282$) (Fig. 5). In addition, loss of both *robo* and *robo2* resulted in a phenotype that closely resembled *robo2* mutants. The average number of microvilli per embryo was

reduced (19 +/−2) (Fig. 4F') and the length was increased as compared to wild type (418 +/− 12nm, n=112) (P = 0.0001) (Fig. 5).

In *slit* mutants, we were able to detect the appropriate number of microvilli on the surface of BCs (33 +/− 3) (Fig. 4A'). In addition, although the microvillus lengths were shorter in *slit* mutants than in wild type (224 +/− 6 nm, n=219) (P<0.0001) (Fig. 5), the length phenotype for *slit* mutants is less severe than what we observed in *robo* mutant embryos (P<0.0001 when microvillus lengths between *robo* and *slit* embryos are compared) (Fig. 5). These data, combined with our observation that *slit* mutants did not have any significant difference in lumen size or shape (Fig. 4A) suggested that either *robo's* function in the LI is at least partially independent of *slit*, or that *slit* mutants may still have some Slit activity. Our data support the latter hypothesis. Since maternal contributions of Slit have been previously reported (Furrer et al., 2007; Bhat et al., 2007; Banerjee et al., 2010), we decided to examine our zygotic *slit* mutant embryos for the presence of maternal *slit* in the HG. *slit* mutant embryos were identified using BP102, which stains the CNS and shows the characteristic collapse phenotype of the CNS axon scaffold observed in *slit* mutants (Kidd et al., 1999). In *slit* embryos, we found that Slit staining persisted in the LI both on the apical surface of boundary cells in the HE, as well as the HVM (Fig. 4B,B'). This was in contrast to *robo* mutants, which had no discernable staining for Robo (Fig. 4D). Our data is consistent with an earlier study that showed a lack of left-right asymmetry defects in the HG of *slit* mutants (Maeda et al., 2007). Because the presence of maternal *slit* in the HG precluded our ability to fully analyze the function of Slit in the HG, we decided to focus on *robo* mutants for our rescue and gain-of-function analysis below.

robo is required in the HVM for correct microvillus length in the HE

Because our antibody staining experiments showed that Robo protein is detected in both the HVM and HE of the LI (Fig 1B, C'), we performed rescue and gain-of-function experiments using the GAL4/UAS system (Brand and Perrimon, 1993) to determine the tissue-specific requirements for *robo's* function in lumen shape and microvillus length. To drive uniform expression in the HE, we used the *byn*-GAL4 driver (Iwaki and Lengyel, 2002). As expected, *byn*-GAL4 drives strong expression of UAS-*robo* in the HE of the LI (Fig. 6B). In wild type embryos overexpression of *robo* in the HE, resulted in lumen shape defects (Fig. 6A) while microvillus length was unaffected (286 +/− 11nm, n=204) (Fig. 5) as compared to wild type. In addition, we did not observe any changes in the expression patterns of Engrailed, Notch or Delta (Fig. S1 D,H,L), demonstrating that increasing *robo* levels in the HE did not alter HG patterning. Moreover, when we used *byn*-GAL4 to drive the expression of UAS-*robo* in *robo* mutant embryos, we did not observe significant rescue of lumen shape (Fig. 6C), or microvillus length (188 +/− 7nm, n=177) as compared to *robo* LOF mutants (Fig. 5).

Next, we tested for the requirement for *robo* in the surrounding HVM. For HVM specific expression we used *Mef2*-GAL4 (Ranganayakulu et al., 1996; Kramer et al., 2001) to drive expression of UAS-*robo* in the HVM (Fig. 6E). We found that while *robo* overexpression in the HVM did not alter lumen shape (Fig. 6D), it did result in a significant increase in microvillus length (405 +/− 11nm, n=192) as compared to wild type (P< 0.0001) (Fig. 5, 6D'). We also examined Notch localization in embryos where *robo* is overexpressed in the HVM. In these embryos, Notch is correctly localized demonstrating that increasing *robo* levels in the HVM does not alter boundary cell fate (data not shown). Finally, when we expressed UAS-*robo* in the HVM of *robo* mutant embryos, we were able to rescue microvillus length to wild type levels (304 +/− 9nm, n=204) (Fig. 5, 6F'). Together, our rescue and gain-of-function results clearly show that Robo is required specifically in the HVM for correct microvilli length in the HE.

The loss of *robo* also leads to defects in the shape of the lumen of the LI (Fig. 4C). However, unlike the microvilli defect, we were unable to rescue lumen shape by driving *robo* expression in either the HE or HVM (Fig. 6C,F). This raises the possibility that either *robo* levels in our rescue backgrounds were not sufficient to rescue the lumen shape defects, or that this phenotype may reflect an earlier requirement for *robo* in HG development that was not provided by the drivers we used for our rescue studies. Still another alternative possibility is that this phenotype is due to a more general loss of adhesion or integrity in the embryo as a result of loss of *robo*, and is secondary to *robo's* specific requirement in the HVM for microvilli length.

DISCUSSION

Our studies show that Robo is specifically required in the HVM for proper microvillus length in the HE. How could Robo in the HVM play a role in regulating the normal lengths of BC microvilli in the underlying HE? It is known that the formation of microvilli requires the assembly of a parallel bundle of actin filaments that maintain their length through the continuous addition of new actin monomers at their barbed ends in the distal tip coupled with disassembly at their pointed ends in the cytoplasm. Increases in microvillus length are thought to correlate with the cytoplasmic concentration of free actin (Stidwill and Burgess, 1986) (for review see (Marshall, 2004)) as well as the association of several actin-binding proteins that regulate actin polymerization (Bartles, 2000). During axon guidance, Robo signaling has been shown to act locally to modulate actin dynamics in the growth cone by influencing the activity of Rho-family GTPases including Cdc42, Rac and RhoA which are thought to function by linking the Robo guidance signal to cytoskeletal rearrangements (for reviews see (Yuan et al., 2003; O'Donnell et al., 2009)). However, this model cannot by itself explain the mechanism by which Robo regulates microvillar growth. While the Slit/Robo signaling pathway has also been shown to influence actin remodeling, it has been shown to do so in a cell autonomous manner. Our results argue that in the hindgut, Robo is influencing microvillar growth from an adjacent tissue, suggesting that its action in regulating actin dynamics in this context is indirect, perhaps by modulation of another signaling pathway that more directly affects actin dynamics and microvillus growth. Several other intercellular signaling pathways, including the Hedgehog and WNT pathways have been implicated in epithelial-mesenchymal crosstalk during villus formation (reviewed in (Spence et al., 2011)).

Another possibility for how Robo signals to the HE from the HVM is through direct interaction with Robo2, which we found localized to the basal HE surface. It was shown that Robo proteins behave as homophilic cell adhesion molecules that are capable of binding to each other via their extracellular domains independent of Slit (Hivert et al., 2002). Our loss of function data argues that *robo2* may function at least in part to antagonize *robo* in the HVM. Loss of *robo2* results in an increase in microvillus lengths that are comparable with what we observe when *robo* is overexpressed in the HVM. The negative regulation of Robo function by related Robo receptors has been demonstrated in vertebrates (Sabatier et al., 2004) and also suggested for Drosophila Robo2 in a more recent study (Evans and Bashaw, 2010). However, our observation that *robo,robo2* double mutants resemble *robo2* mutants suggests a more complex role for *robo2* in the HE than simply to antagonize *robo* in the HVM.

Our studies are consistent with the fact that Robo does not seem to be required to form microvilli, but rather regulates microvilli length once they are formed. Interestingly, the effect of Robo on microvillus growth shares some similarities with that of two other membrane proteins, the non-classical cadherin Cad99C and the ERM protein Ezrin. Cad99C, which is regulated by Hedgehog signaling (Schlichting et al., 2005), localized to

microvilli and has a dose dependent effect on microvilli length in *Drosophila* ovarian follicle cells (D'Alterio et al., 2005; Schlichting et al., 2006). Similarly, studies in mouse have shown that phosphorylation of Ezrin, a protein that has been shown to link actin dynamics to the plasma membrane enhances microvillus length in a mouse hepatic cell line (Lan et al., 2006). In *Drosophila*, both Cad99C and the sole ERM protein Moesin, appear to be enriched on the apical surface of the HE (McCartney and Fehon, 1996; Fung et al., 2008) suggesting that they may also function in regulating microvillus length in the HG and could be possible targets of Robo signaling from the HVM.

Our protein localization data show that in addition to the HVM, Slit is also localized to the apical surface of BCs in the HE where the microvilli form. Our analysis of *slit* and *robo* embryos shows that BC microvilli length is reduced in both mutant backgrounds (Fig. 5). However, we are puzzled by the fact that we do not detect Robo or Robo2 protein on this surface, and that our data show that *robo* is specifically required in the HVM not the HE for controlling microvillus length. In addition, we still observe Slit localization to the BCs in the absence of Robo (data not shown). What is the function for Slit in the BCs and is Slit functioning independently of Robo in this process? The presence of maternal Slit protein in our *slit* loss-of-function embryos precludes our ability to answer this question at this time. One possible avenue for further study is the possibility that Slit may also be required in the HE for maintenance of microvillar structures in the larva through a separate mechanism.

Finally, is the role for Slit/Robo signaling in microvilli formation specific to the *Drosophila* intestine or could the role for this pathway in microvilli development be conserved in vertebrates? Further study is required to confirm this possibility. However it is interesting to note that Slit homologues are expressed in the developing mouse intestine from E11.5 and E13.5 (Holmes et al., 1998), which correlates well with the time of active intestinal microvillar formation (Pinson et al., 1998), as well as in the mesenchyme of the developing chick intestine (Holmes and Niswander, 2001). In addition, co-expression of Slit2 and Robo1 proteins has been reported in human placental villi (Liao et al.).

Conclusion

In this study, our aim was to examine the localization and function of the *slit* and *robo* genes in the *Drosophila* embryonic HG. Our results showed that loss of *slit* or *robo* does not result in defects in overall HG patterning but does result in a decrease in microvillus length on the BCs of the HE. We also show using rescue and gain-of-function assays that *robo* is specifically required in the surrounding HVM for microvillus growth in the HE. Furthermore, we provide evidence that *robo2* may function in part to antagonize the function of *robo* during this process. These results not only represent a novel, non-cell autonomous role for Robo proteins in microvillus growth, but also provide molecular insight into the long established findings that the mesenchyme plays an important role in directing microvilli growth in the underlying epithelium.

EXPERIMENTAL PROCEDURES

Fly Strains and Genetics

Fly crosses and experiments were performed at 25°C. The w^{1118} strain was used as the wild type. The following mutations have been described previously: *robo* (*robo*^{Z570}), *robo2* (*robo2*^{X123}), *robo,robo2*, (Simpson et al., 2000b), *slit* (sli^{2}) (Kidd et al., 1999). UAS-*robo* was also described previously (Kramer et al 2001). The GAL4-UAS system (Brand and Perrimon, 1993) was used to drive expression of the *robo* transgene with *Mef2*-GAL4 (Ranganayakulu et al., 1996)(Kramer et al., 2001) or *byn-GAL4 and byn-GAL4;UAS-eGFP* (gifts from David Iwaki) for the gain-of-function experiments. For the HVM rescue

experiment, UAS-*robo*;*robo*^{z570}/*Cyo,twist-GFP* virgin females were crossed with *robo*^{Z570}/*Cyo,twist-GFP; Mef*-GAL4 to get UAS-*robo*; *robo*^{z570}/ *robo*^{z570}; *Mef*GAL4/+ embryos. For the HE rescue experiment, UAS-*robo*; *robo*^{z570}/*Cyo,twist-GFP* were crossed with *robo*^{z570}/*Cyo,twist-GFP; byn-GAL4,* UAS-*eGFP/TM6,* to get UAS-*robo*; *robo*^{z570}/ *robo*^{z570}; *byn*-GAL4, UAS-*eGFP* embryos.

Immunofluorescence

Embryos were fixed and stained according to standard protocols as described previously (Kramer et al., 2001). The following antibodies were used: mouse anti-Slit N + C (C555.6D) (1:10 for each epitope), mouse anti-Robo 13C9 (1:20), rabbit anti-Robo2 (1:400), FITC anti-mouse (1:500), Cy5 anti– mouse (1:500) and Cy3 anti-mouse (1:500) (Invitrogen). The anti-Engrailed (1:10), anti-Delta (1:10), anti-NICD (Notch-Intracelluar Domain) (1:10), and anti-Crumbs (1:10) (developed by C. Goodman, S. Artavanis-Tsakonas, and E. Knust respectively) were obtained from the Developmental Studies Hybridoma Bank developed under the auspices of the NICHD and maintained by The University of Iowa, Department of Biology, Iowa City, IA 52242. Embryos were cleared in 60% Glycerol in PBS and mounted whole or as transverse sections cut with a double-edged feather razor blade (Ted Pella). Confocal z sections were collected at ambient temperature on an inverted microscope (IX81; Olympus) with a CARV2 Nipkow disc confocal unit (BD Biosciences) equipped with a UApo/340 40± 1.15 NA, or UPlanApo 60± 1.2 NA water immersion objective (Olympus) and a Hamamatsu Orca EM-CCD camera. Image processing and analysis was done with iVision image analysis software (BD Biosciences) and Photoshop CS2 (Adobe).

Electron Microscopy

Mutant embryos were selected based on the absence of a GFP-marked balancer chromosome. Embryos were fixed and embedded as described previously (Soplop et al., 2009), except for sections shown in Figs 3D and E. The ultrastructure of the HVM/HE interface was best preserved using the following modified procedure: Embryos were fixed for 30 minutes at room temperature in 4% Paraformaldehyde and 2% Glutaraldehyde in 0.1M Cacodylate Buffer, pH 7.4, and Heptane. Embryos were hand devitellinized, rinsed in 0.1M Cacodylate Buffer, pH 7.4, and then post-fixed, embedded and sectioned as described (Soplop et al., 2009).

Immuno-electron microscopy

Embryos were dechorionated with bleach and fixed for 30 minutes in 4% Paraformaldehyde, 0.25% Glutaraldehyde in 100mM Cacodylate buffer, pH7 and 5ml Heptane. Following devitellinization with methanol, embryos were rehydrated in 100mM Phosphate Buffer and 0.05% Saponin. To stabilize carbohydrate moieties, embryos were incubated in 75mM Lysine, 10.5mM sodium meta-periodate, 75mM Phosphate, pH7.4, for 30 minutes. Slit antibody was prepared in a blocking solution at a 1:10 dilution containing 100mM Phosphate Buffer, pH 7.4, 0.05% Saponin, 1mg/ml BSA, 50mM Glycine and 5% NGS. Following standard washes, embryos were incubated at room temperature for 1.5 hours with biotin anti-Mouse secondary (1:500) (Jackson ImmunoResearch) followed by Alexa Flour 488 FlouroNanogold conjugated Steptavidin (1:10) (Nanoprobes). Integrity of embryos were stabilized using 2% Glutaraldehyde and 100mM Cacodylic Acid, pH 7 for 30 minutes at room temperature, washed to remove fixative, and rinsed with distilled water. The Nanogold particle was developed using HQ Silver Enhancement Reagent (Nanoprobes) allowing the reaction to proceed for 15 minutes. Post-fixation, embedding and cutting were performed as described (Soplop et al., 2009).

Statistical Analysis

Microvillus length and length of the apical surface of the HG were measured as number of pixels using iVision image analysis software (BD Biosciences) and then converted to nm using the distance bar on each micrograph image obtained using Image Capture Engine V600 software (Advanced Microscope Techniques). Microsoft Excel was used for managing raw data. We used GraphPad PRISM software to evaluate the statistical relevance of microvilli lengths, number of nuclei per TEM, and length of the HG apical surface. This data is expressed as means +/− SE. Statistical relevance was evaluated using unpaired Student t-tests. Means were significantly different when $P<0.05$ for a two-tailed test.

Supplementary Material

Refer to Web version on PubMed Central for supplementary material.

Acknowledgments

We thank R. Patel for assistance with EM, R. Foty for help with statistical analysis, D. Iwaki for providing the *byn*-GAL4 line, J. Canabal for technical assistance, and members of the Kramer lab for critical reading of this manuscript. We also thank the Developmental Studies Hybridoma Bank and the Bloomington stock center for providing antibodies and fly stocks. This study was supported by a National Science Foundation grant (award ID 0744165), and a National Institutes of Health grant (5R01AR054482 from NIH/NIAMS) to S.G. Kramer.

Grant Sponsor: National Science Foundation; Grant Number: 0744165

REFERENCES

Banerjee S, Blauth K, Peters K, Rogers SL, Fanning AS, Bhat MA. Drosophila neurexin IV interacts with Roundabout and is required for repulsive midline axon guidance. J Neurosci. 2010; 30:5653–5667. [PubMed: 20410118]

Bartles JR. Parallel actin bundles and their multiple actin-bundling proteins. Curr Opin Cell Biol. 2000; 12:72–78. [PubMed: 10679353]

Bhat KM, Gaziova I, Krishnan S. Regulation of axon guidance by slit and netrin signaling in the Drosophila ventral nerve cord. Genetics. 2007; 176:2235–2246. [PubMed: 17565966]

Brand AH, Perrimon N. Targeted gene expression as a means of altering cell fates and generating dominant phenotypes. Development. 1993; 118:401–415. [PubMed: 8223268]

Brose K, Bland KS, Wang KH, Arnott D, Henzel W, Goodman CS, Tessier-Lavigne M, Kidd T. Slit proteins bind Robo receptors and have an evolutionarily conserved role in repulsive axon guidance. Cell. 1999; 96:795–806. [PubMed: 10102268]

Brown JW, McKnight CJ. Molecular model of the microvillar cytoskeleton and organization of the brush border. PLoS One. 2010; 5:e9406. [PubMed: 20195380]

Campos-Ortega, JA.; Hartenstein, V. The embryonic development of *Drosophila melanogaster*. Springer Verlag; Berlin Heidelberg: 1997.

D'Alterio C, Tran DD, Yeung MW, Hwang MS, Li MA, Arana CJ, Mulligan VK, Kubesh M, Sharma P, Chase M, Tepass U, Godt D. Drosophila melanogaster Cad99C, the orthologue of human Usher cadherin PCDH15, regulates the length of microvilli. J Cell Biol. 2005; 171:549–558. [PubMed: 16260500]

Evans TA, Bashaw GJ. Functional diversity of Robo receptor immunoglobulin domains promotes distinct axon guidance decisions. Curr Biol. 2010; 20:567–572. [PubMed: 20206526]

Fung S, Wang F, Chase M, Godt D, Hartenstein V. Expression profile of the cadherin family in the developing Drosophila brain. J Comp Neurol. 2008; 506:469–488. [PubMed: 18041774]

Furrer MP, Vasenkova I, Kamiyama D, Rosado Y, Chiba A. Slit and Robo control the development of dendrites in Drosophila CNS. Development. 2007; 134:3795–3804. [PubMed: 17933790]

Fuss B, Hoch M. Notch signaling controls cell fate specification along the dorsoventral axis of the Drosophila gut. Curr Biol. 2002; 12:171–179. [PubMed: 11839268]

Grevengoed EE, Fox DT, Gates J, Peifer M. Balancing different types of actin polymerization at distinct sites: roles for Abelson kinase and Enabled. J Cell Biol. 2003; 163:1267–1279. [PubMed: 14676307]

Heintzelman MB, Mooseker MS. Assembly of the intestinal brush border cytoskeleton. Curr Top Dev Biol. 1992; 26:93–122. [PubMed: 1563281]

Hivert B, Liu Z, Chuang CY, Doherty P, Sundaresan V. Robo1 and Robo2 are homophilic binding molecules that promote axonal growth. Mol Cell Neurosci. 2002; 21:534–545. [PubMed: 12504588]

Holmes G, Niswander L. Expression of slit-2 and slit-3 during chick development. Dev Dyn. 2001; 222:301–307. [PubMed: 11668607]

Holmes GP, Negus K, Burridge L, Raman S, Algar E, Yamada T, Little MH. Distinct but overlapping expression patterns of two vertebrate slit homologs implies functional roles in CNS development and organogenesis. Mech Dev. 1998; 79:57–72. [PubMed: 10349621]

Iwaki DD, Johansen KA, Singer JB, Lengyel JA. drumstick, bowl, and lines are required for patterning and cell rearrangement in the Drosophila embryonic hindgut. Dev Biol. 2001; 240:611–626. [PubMed: 11784087]

Iwaki DD, Lengyel JA. A Delta-Notch signaling border regulated by Engrailed/Invected repression specifies boundary cells in the Drosophila hindgut. Mech Dev. 2002; 114:71–84. [PubMed: 12175491]

Karagiosis SA, Ready DF. Moesin contributes an essential structural role in Drosophila photoreceptor morphogenesis. Development. 2004; 131:725–732. [PubMed: 14724125]

Kedinger M, Simon-Assmann PM, Lacroix B, Marxer A, Hauri HP, Haffen K. Fetal gut mesenchyme induces differentiation of cultured intestinal endodermal and crypt cells. Dev Biol. 1986; 113:474–483. [PubMed: 2868951]

Kidd T, Bland KS, Goodman CS. Slit is the midline repellent for the robo receptor in Drosophila. Cell. 1999; 96:785–794. [PubMed: 10102267]

Kramer SG, Kidd T, Simpson JH, Goodman CS. Switching repulsion to attraction: changing responses to slit during transition in mesoderm migration. Science. 2001; 292:737–740. [PubMed: 11326102]

Kraut R, Zinn K. Roundabout 2 regulates migration of sensory neurons by signaling in trans. Curr Biol. 2004; 14:1319–1329. [PubMed: 15296748]

Lan M, Kojima T, Murata M, Osanai M, Takano K, Chiba H, Sawada N. Phosphorylation of ezrin enhances microvillus length via a p38 MAP-kinase pathway in an immortalized mouse hepatic cell line. Exp Cell Res. 2006; 312:111–120. [PubMed: 16274688]

Lengyel JA, Iwaki DD. It takes guts: the Drosophila hindgut as a model system for organogenesis. Dev Biol. 2002; 243:1–19. [PubMed: 11846473]

Liao WX, Wing DA, Geng JG, Chen DB. Perspectives of SLIT/ROBO signaling in placental angiogenesis. Histol Histopathol. 25:1181–1190. [PubMed: 20607660]

Lin HW, Schneider ME, Kachar B. When size matters: the dynamic regulation of stereocilia lengths. Curr Opin Cell Biol. 2005; 17:55–61. [PubMed: 15661519]

Maeda R, Hozumi S, Taniguchi K, Sasamura T, Murakami R, Matsuno K. Roles of single-minded in the left-right asymmetric development of the Drosophila embryonic gut. Mech Dev. 2007; 124:204–217. [PubMed: 17241775]

Marshall WF. Cellular length control systems. Annu Rev Cell Dev Biol. 2004; 20:677–693. [PubMed: 15473856]

Mathan M, Hermos JA, Trier JS. Structural features of the epithelio-mesenchymal interface of rat duodenal mucosa during development. J Cell Biol. 1972; 52:577–588. [PubMed: 5009520]

McCartney BM, Fehon RG. Distinct cellular and subcellular patterns of expression imply distinct functions for the Drosophila homologues of moesin and the neurofibromatosis 2 tumor suppressor, merlin. J Cell Biol. 1996; 133:843–852. [PubMed: 8666669]

McLin VA, Henning SJ, Jamrich M. The role of the visceral mesoderm in the development of the gastrointestinal tract. Gastroenterology. 2009; 136:2074–2091. [PubMed: 19303014]

Medioni C, Astier M, Zmojdzian M, Jagla K, Semeriva M. Genetic control of cell morphogenesis during Drosophila melanogaster cardiac tube formation. J Cell Biol. 2008; 182:249–261. [PubMed: 18663140]

Murakami R, Shiotsuki Y. Ultrastructure of the hindgut of Drosophila larvae, with special reference to the domains identified by specific gene expression patterns. J Morphol. 2001; 248:144–150. [PubMed: 11304745]

O'Donnell M, Chance RK, Bashaw GJ. Axon growth and guidance: receptor regulation and signal transduction. Annu Rev Neurosci. 2009; 32:383–412. [PubMed: 19400716]

Pinson KI, Dunbar L, Samuelson L, Gumucio DL. Targeted disruption of the mouse villin gene does not impair the morphogenesis of microvilli. Dev Dyn. 1998; 211:109–121. [PubMed: 9438428]

Ranganayakulu G, Schulz RA, Olson EN. Wingless signaling induces nautilus expression in the ventral mesoderm of the Drosophila embryo. Dev Biol. 1996; 176:143–148. [PubMed: 8654890]

Ratineau C, Duluc I, Pourreyron C, Kedinger M, Freund JN, Roche C. Endoderm- and mesenchyme-dependent commitment of the differentiated epithelial cell types in the developing intestine of rat. Differentiation. 2003; 71:163–169. [PubMed: 12641570]

Roberts DJ. Molecular mechanisms of development of the gastrointestinal tract. Dev Dyn. 2000; 219:109–120. [PubMed: 11002332]

Rothberg JM, Jacobs JR, Goodman CS, Artavanis-Tsakonas S. slit: an extracellular protein necessary for development of midline glia and commissural axon pathways contains both EGF and LRR domains. Genes Dev. 1990; 4:2169–2187. [PubMed: 2176636]

Sabatier C, Plump AS, Le M, Brose K, Tamada A, Murakami F, Lee EY, Tessier-Lavigne M. The divergent Robo family protein rig-1/Robo3 is a negative regulator of slit responsiveness required for midline crossing by commissural axons. Cell. 2004; 117:157–169. [PubMed: 15084255]

San Martin B, Bate M. Hindgut visceral mesoderm requires an ectodermal template for normal development in Drosophila. Development. 2001; 128:233–242. [PubMed: 11124118]

Santiago-Martinez E, Soplop NH, Patel R, Kramer SG. Repulsion by Slit and Roundabout prevents Shotgun/E-cadherin-mediated cell adhesion during Drosophila heart tube lumen formation. J Cell Biol. 2008; 182:241–248. [PubMed: 18663139]

Saotome I, Curto M, McClatchey AI. Ezrin is essential for epithelial organization and villus morphogenesis in the developing intestine. Dev Cell. 2004; 6:855–864. [PubMed: 15177033]

Schlichting K, Demontis F, Dahmann C. Cadherin Cad99C is regulated by Hedgehog signaling in Drosophila. Dev Biol. 2005; 279:142–154. [PubMed: 15708564]

Schlichting K, Wilsch-Brauninger M, Demontis F, Dahmann C. Cadherin Cad99C is required for normal microvilli morphology in Drosophila follicle cells. J Cell Sci. 2006; 119:1184–1195. [PubMed: 16507588]

Simpson JH, Bland KS, Fetter RD, Goodman CS. Short-range and long-range guidance by Slit and its Robo receptors: a combinatorial code of Robo receptors controls lateral position. Cell. 2000a; 103:1019–1032. [PubMed: 11163179]

Simpson JH, Kidd T, Bland KS, Goodman CS. Short-range and long-range guidance by slit and its Robo receptors. Robo and Robo2 play distinct roles in midline guidance. Neuron. 2000b; 28:753–766. [PubMed: 11163264]

Skaer, H. The Alimentary canal. In: Bate, M.; Arias, AM., editors. The Development of *Drosophila melanogaster*. Vol. II. Cold Spring Harbor Laboratory Press; New York: 1993. p. 941-1012.

Soplop NH, Patel R, Kramer SG. Preparation of embryos for electron microscopy of the Drosophila embryonic heart tube. J Vis Exp. 2009

Spence JR, Lauf R, Shroyer NF. Vertebrate intestinal endoderm development. Dev Dyn. 2011; 240:501–520. [PubMed: 21246663]

Stidwill RP, Burgess DR. Regulation of intestinal brush border microvillus length during development by the G- to F-actin ratio. Dev Biol. 1986; 114:381–388. [PubMed: 3956872]

Takashima S, Yoshimori H, Yamasaki N, Matsuno K, Murakami R. Cell-fate choice and boundary formation by combined action of Notch and engrailed in the Drosophila hindgut. Dev Genes Evol. 2002; 212:534–541. [PubMed: 12459922]

Tepass U, Hartenstein V. The development of cellular junctions in the Drosophila embryo. Dev Biol. 1994; 161:563–596. [PubMed: 8314002]

Tepass U, Theres C, Knust E. crumbs encodes an EGF-like protein expressed on apical membranes of Drosophila epithelial cells and required for organization of epithelia. Cell. 1990; 61:787–799. [PubMed: 2344615]

Yuan XB, Jin M, Xu X, Song YQ, Wu CP, Poo MM, Duan S. Signalling and crosstalk of Rho GTPases in mediating axon guidance. Nat Cell Biol. 2003; 5:38–45. [PubMed: 12510192]

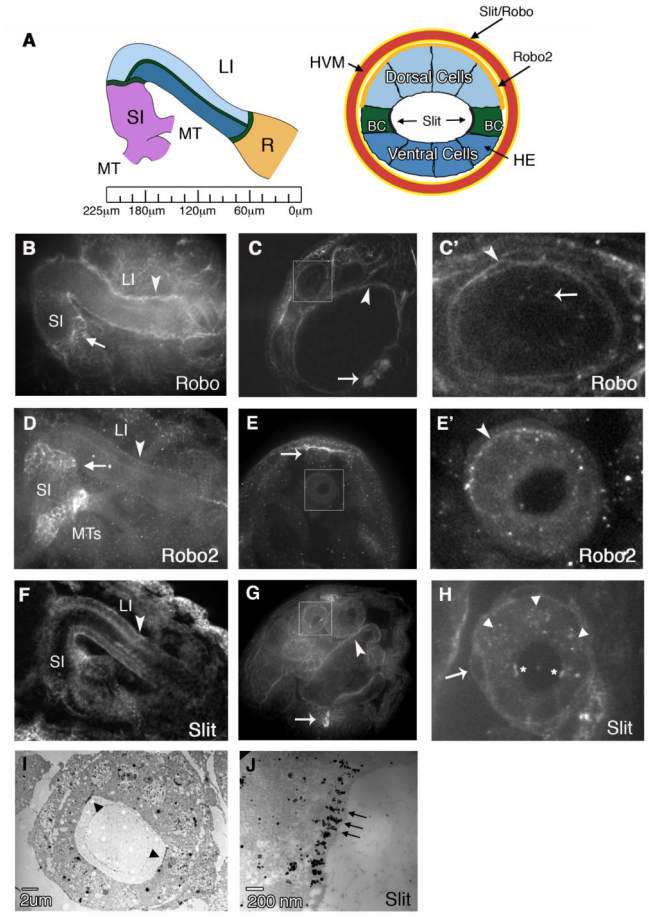

Figure 1.

Localization of Slit and Robo2 in the embryonic hindgut. (A) Left: schematic showing hindgut (HG) organization in stage 16 embryos. The hindgut begins at the anterior end of the embryo (left) with the small intestine (SI) and is separated from both the large Intestine (LI) and Rectum(R) by a ring of Boundary Cells (green lines). The renal (Malpighian) tubules (MT) connect to the HG near the SI. Ruler shows distance (in µm) from the most posterior point of the embryo. Right: cross section through the LI reveals the Dorsal, Ventral and Boundary Cells (BC) comprising the HG epithelium (HE), which is surrounded by the HG visceral mesoderm (HVM) (red). Robo2 is localized to the basal surface of the HE Dorsal cells (orange), while Slit and Robo are localized to the surfaces of the HVM (yellow). Slit is also localized to the apical surface of the BCs (black). (B) Whole mount embryo showing Robo in the SI, LI and HVM (arrowhead). Arrow points to the region where the MTs connect to the SI. (C) In cross-section, Robo staining can be seen in the ventral CNS (arrow) and the midgut visceral mesoderm (arrowhead). The large intestine of the hindgut is boxed and enlarged in (C') to show Robo staining on the surface of the HVM (arrowhead) and in cytoplasmic puncta in the HE (arrow). (D) Robo2 localizes to the LI (arrowhead) and the base of the MTs in the SI. High levels of Robo2 are also seen at the boundary between the SI and LI (arrow). (E) In cross-section, Robo2 staining can be seen in the dorsal vessel (arrow). The HG LI is boxed and enlarged in (E') to show Robo2 staining on the basal surface of the Dorsal HE (arrowhead). (F) Anti-Slit staining in whole mount shows Slit in the SI, LI and HVM (arrowhead). (G) In cross section, Slit staining is seen in the ventral midline glia (arrow) and the midgut visceral mesoderm (arrowhead). (H) Cross-sectioned embryo stained with Slit and Engrailled to show Slit localization on the surface of

the HVM (arrow) as well as in cytoplasmic puncta in the HE. Arrowheads show Engrailed staining in the nuclei of Dorsal cells. Asterisks indicate Slit localization to the apical surface of the BCs. (I) Slit immuno-EM of a thin section of the LI. Arrowheads point to BCs. (J) Close-up of one BC showing electron-dense Slit staining on the BC surface. All embryos are at stage 16.

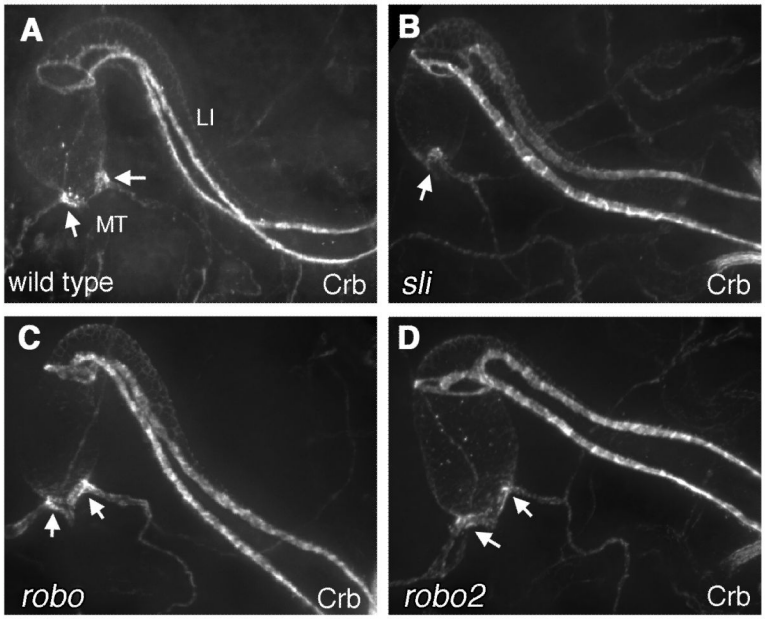

Figure 2.

HG shape and patterning in *slit, robo* and *robo2* mutants. (A-D) Crb staining in the hindgut of wild type (A), $slit^2/slit^2$ (B), $robo^{z570}/robo^{z570}$ (C), or $robo2^{x123}/robo2^{x123}$ embryos. The apical localization of Crb in the BCs of the large intestine is unaffected in *slit, robo, and robo2* mutants. In addition, the Malpighian tubules (MT) are properly positioned in all mutant backgrounds (arrows). In (B) the second set of MTs are present but out of the plane of focus.

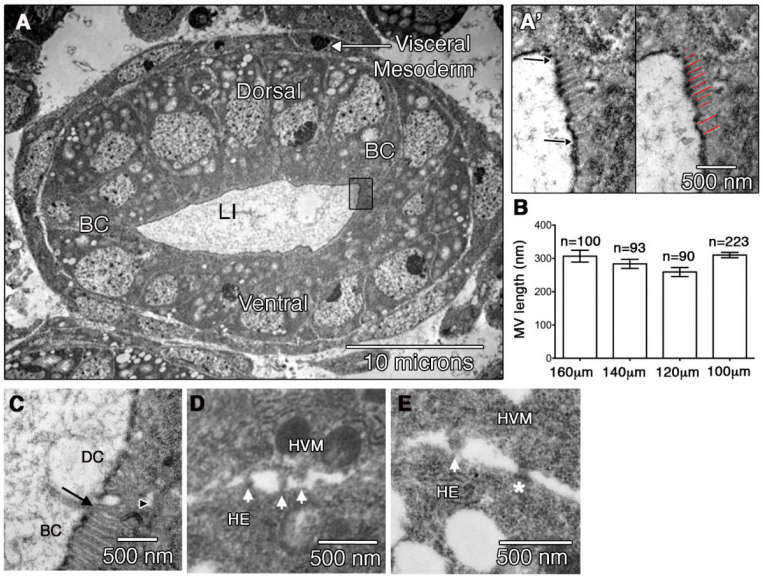

Figure 3.

Characterization of HG morphology in wild type embryos. (A) TEM showing the Dorsal, Ventral and Boundary Cells (BC) of a wild type HE, surrounded by the visceral mesoderm (arrow). Boxed region shows the apical surface of a BC that is magnified in (A'). In left panel, area between arrows delineates the apical membrane of the BC where microvilli are found. The apical surface of hindgut epithelium is covered by layers of cuticle that are visible as a dark line by TEM. On right, red lines indicate where individual microvillus length is measured. (B) Graph depicting microvilli lengths at regular intervals across the HG (refer to Figure 1A). n=number of microvilli analyzed. (C) An example of the apical surface of the HE at the interface of a BC and a dorsal cell (DC). Arrow points to the border between these two cells. Arrowhead indicates an adherens junction. BC microvilli are regularly spaced with a visible F-actin bundle, while the membranous protrusions of Dorsal cells are irregularly shaped with uneven spacing. (D-E). TEMs of embryos in cross-section showing the area where the HVM and HE come into contact. Arrow points to membrane protrusions. Asterisk in (E) shows an adherens junction.

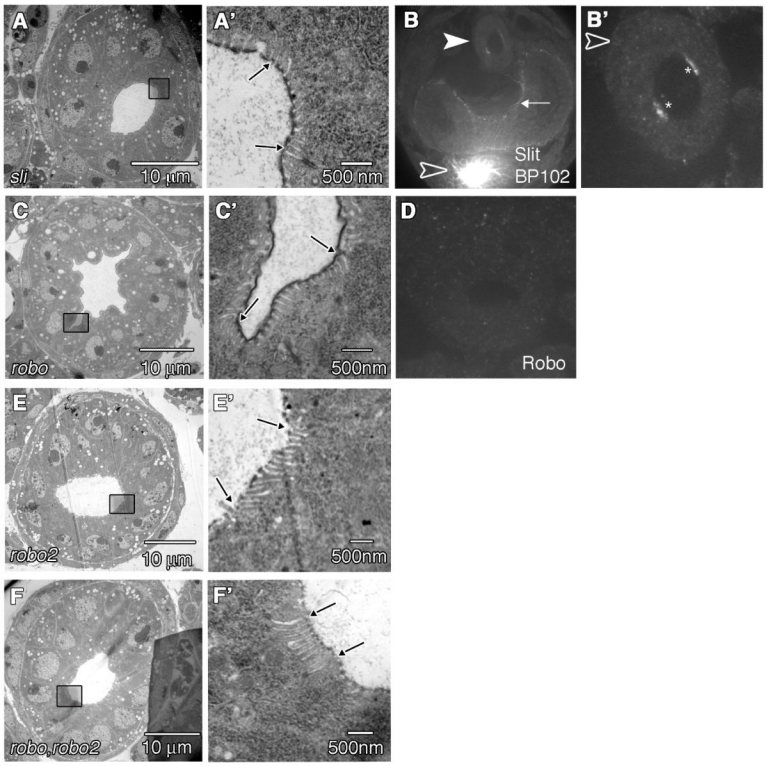

Figure 4.

slit, robo and *robo2* mutant phenotypes in the HG. (A) TEM section through the LI of a $slit^2/slit^2$ embryo. (A') Magnified view of boxed region in (A) reveals the apical surface of a BC's. Arrows indicate BC borders. (B) Anti-Slit staining in a $slit^2/slit^2$ embryo. Embryos were co-stained with anti-BP102 to identify *slit* mutants based on the axonal collapse phenotype in the CNS (empty arrowhead). Arrow points to Slit staining in the visceral mesoderm in *slit* mutant embryos. Filled arrowhead points to the LI. (B') Magnified view of the LI from the same embryo as in (B). Asterisks show anti-Slit staining on the apical surface of BCs. Arrowhead points to low levels of Slit staining in the HVM. (C) TEM section through the LI of a $robo^{z570}/robo^{z570}$ embryo. (C') Magnified view of boxed region in (C) reveals the apical surface of a BC. Arrows indicate BC borders. (D) anti-Robo staining in a cross-sectioned $robo^2/robo^2$ embryo showing little to no staining in the LI. (E) TEM section through the LI of a $robo2^{x123}/robo2^{x123}$ embryo. (E') Magnified view of boxed region in (E) reveals the apical surface of a BC. The borders of the BC are indicated with arrows. (F) TEM section through the LI of a *robo,robo2* double mutant embryo. (F') Magnified view of boxed region in (F) reveals the apical surface of a BC. The borders of the BC are indicated with arrows.

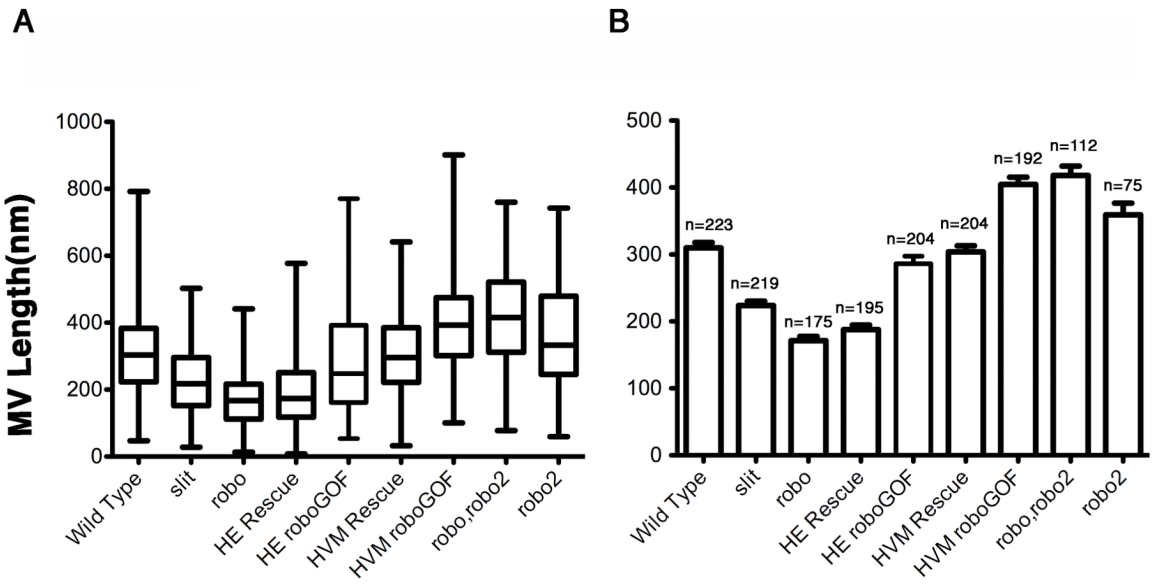

Figure 5.

robo affects BC microvilli length in a dose dependant manner. (A) Box plot: Box represents values within the 25th to 75th percentile. The line within the box represents the median value. Whiskers illustrate minimum and maximum values. (B) Data shown as mean +/− SEM. n=number of microvilli analyzed. Statistical relevance was evaluated using unpaired Student t-tests. Biological significance was determined when P<0.05 for a two-tailed test. Both *slit*^{2}/slit^{2} and *robo*^{z570}/robo^{z570} embryos had reduced microvillus lengths when compared to wild type (P<0.0001 for both genotypes when compared to wild type). In addition, microvillus lengths in *slit*^{2}/slit^{2} embryos were less severe than *robo*^{z570}/robo^{z570} embryos (P<0.0001). Overexpression of *robo* in the HE (HE roboGOF) did not result in a significant change in microvillus lengths compared to wild type. Expression of *robo* in the HE of an embryo lacking endogenous *robo* (HE Rescue) had shorter microvillus lengths that were not significantly different from *robo* mutant embryos, while expression of *robo* in the HVM in an embryo lacking endogenous *robo* (HVM Rescue) restored microvillus length to that seen in wild type. Overexpression of *robo* in the HVM (HVM roboGOF) resulted in a significant increase in microvillus length when compared to wild type (P<0.0001). Similarly, loss of *robo2* or both *robo* and *robo2* resulted in significant increases in microvillus lengths as compared with wild type (P<0.05) and (P<0.0001) respectively.

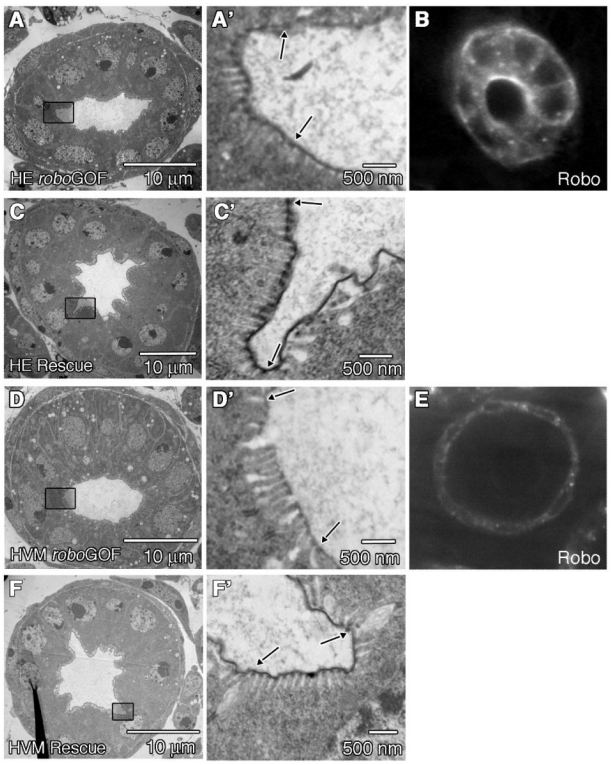

Figure 6.

Robo is required in the HVM for correct microvilli length. (A,C,D,F) are TEM sections through the LI of stage 16 embryos, and (A',C',D',F') are zoomed in areas of the apical surface of the BCs (outlined by boxes in (A,C,D,F). Arrows indicate borders of the BC. (A,A') UAS-*robo/byn*-GAL4 embryo, in which *robo* is overexpressed in the HE. Microvillus lengths and lumen shape are not significantly affected. (B) Anti-Robo staining in a UAS-*robo/byn*-GAL4 embryo shown in cross section. As expected, high levels of Robo staining can be seen in the cells of the HE. (C,C') UAS-*robo*; $robo^{z570}/robo^{z570}$;*byn*-GAL4/+ embryo. Expression of *robo* in the HE of *robo* mutant embryos does not rescue lumen shape or microvilli length ($P<0.0001$ when comparing microvillus lengths between embryos expressing *robo* only in the HE, and wild type.) (D,D') UAS-*robo*/*Mef2*-GAL4 embryo, in which *robo* is overexpressed in the HVM. Lumen shape is not affected (D) but the microvilli are significantly longer than wild type ($P<0.0001$ when comparing microvillus lengths in embryos where *robo* is overexpressed in the HVM, and wild type) (D'). (E) Anti-Robo staining in a UAS-*robo*/*Mef2*-GAL4 embryo. As expected, high levels of Robo staining can be seen in the cells of the HVM. (F,F') UAS-*robo*;$robo^{z570}/robo^{z570}$;*Mef2*-GAL4/+ embryo. Expression of *robo* in the HVM in a *robo* mutant rescues microvilli length (F') but does not rescue lumen shape (F).